

THz Device Design for SiGe HBT under Sub-room Temperature to Cryogenic Conditions

Dinesh Gupta
Department of Electrical Engineering
IIT Hyderabad
Sangareddy, Telangana, 502285, India
ee16resch11007@iith.ac.in

Oves Badami
Department of Electrical Engineering
IIT Hyderabad
Sangareddy, Telangana, 502285, India
oves.badami@ee.iith.ac.in

Sankatali Venkateswarlu
Department of Electrical Engineering
IIT Hyderabad
Sangareddy, Telangana, 502285, India
ee15resch11007@iith.ac.in

Kaushik Nayak
Department of Electrical Engineering
IIT Hyderabad
Sangareddy, Telangana, 502285, India
knayak@ee.iith.ac.in

Abstract— BiCMOS technology can be a possible replacement for FDSOI and FinFET technology due to their higher transconductance, which allows them to operate at in THz range i.e. radio frequencies (RF) in addition to their higher voltage handling ability. The most advanced SiGe heterojunction bipolar transistor (HBT) technology (55-nm BiCMOS) demonstrates room temperature cut-off frequency (f_t) and maximum oscillation frequency (f_{max}) of 320 GHz and 370 GHz respectively. In this paper, we performed TCAD analysis to investigate the performance metrics, f_t and f_{max} of the SiGe HBT at different cryogenic temperatures. The calibrated Gummel characteristics reveals that a record DC current gain of 1.2×10^4 is obtained at 77 K for $V_{BE} = V_{CE} = 1.2$ V. The HBT device employs bandgap engineering by linearly varying the Ge concentration in the base region, which enhances the device performance. Both the bandgap engineering with linearly graded Germanium (Ge) profile (induces intrinsic drift field in the base) and the cryogenic operation of the HBT device results in enhancement of f_t and f_{max} . Our simulations predict that the value of peak f_t decreases below 100 K due to increase in the emitter junction capacitance and the peak f_{max} increase is due to decrease in collector junction capacitance and base resistance. The aggregate metric $f_t + f_{max} > 1.2$ THz is achieved under cryogenic condition without scaling the device, this advantage can be utilized in the THz device applications.

Keywords—THz, BiCMOS, SiGe, HBT, Cryogenic temperature, f_t , f_{max} , current gain, Gummel-characteristics, bandgap engineering.

I. INTRODUCTION

The number of applications for devices that can operate at RF has increased dramatically off-late. This has intensified the device engineering in the microwave transistors so as to improve their performance and make them integrable with state-of-the-art CMOS devices. These devices have applications in 5G communications, radar, automotive industry where the devices are often subjected to harsh environmental conditions [1]. However, the limitations in scaling of the high speed CMOS devices (due to poor electrostatics integrity and high parasitics) have forced industry to move towards BiCMOS technology. In high-speed analog and communication circuits, SiGe based HBT have appeared to be a very promising candidate [1]-[3]. Another important application for SiGe based HBT is quantum computing where devices have to operate at cryogenic

temperatures [2], [4]. H. Ying et al. have demonstrated the successful DC operation of SiGe HBTs down to extremely low cryogenic temperature of 70 mK [3]. A challenging application that has been addressed with cryogenic SiGe HBTs is the amplification of extremely weak signals in radio astronomy [5]-[6]. When SiGe HBT devices are cooled, the small-signal AC performance metrics (f_t and f_{max}) and DC parameters [current gain (β), transconductance (g_m), early voltage (V_A), etc.] are expected to be enhanced further and this is the topic of this contribution.

II. DEVICE DESIGN AND SIMULATION METHODOLOGY

A 2D TCAD structure of n-p-n SiGe HBT that is used in this work is shown in Fig. 1. Linearly varying Ge mole fraction in $Si_{1-x}Ge_x$ base has been used in the base region [7],[14]. The maximum Ge molefraction is set to $x = 0.26$, at the collector base junction. Two extrinsic base contacts have been designed to reduce the current crowding effect as well as reduced base link resistance with the intrinsic base in the device structure[15]-[17]. SiGe base region below the emitter window boron doping with Gaussian profile used. The peak doping of $Si_{1-x}Ge_x$ base was set to $9.9 \times 10^{19} \text{ cm}^{-3}$. We used thermal boundary outside the device structure in order to consider cryogenic environment. The design of SiGe HBT structure with dimension and average (Avg.) doping profile have been mentioned in the Table I. In our simulations, we have incorporated hydrodynamic carrier transport model along with Shockley-Read-Hall (SRH) recombination, temperature dependent carrier-carrier scattering, field, temperature and doping dependent carrier mobility models to capture the device physics.

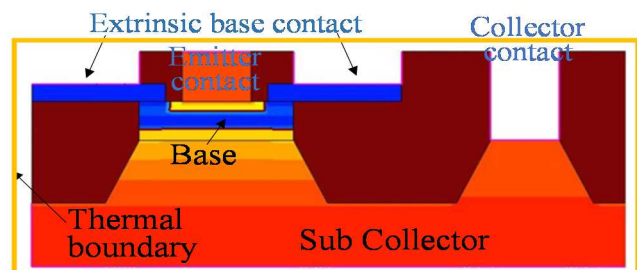


Fig. 1. Schematic representation of simulated SiGe HBT.

TABLE I. PARAMETERS USED FOR SIGE HBT DESIGN.

Avg. Emitter Doping (N_E) (cm^{-3})	Avg. Base Doping (N_B) (cm^{-3})	Avg. Collector Doping (N_C) (cm^{-3})	Emitter Width (W_E) (nm)	Base width (W_B) (nm)	Collector Width (W_C) (nm)
1.5×10^{20}	9.9×10^{19}	3×10^{17}	8	25	375

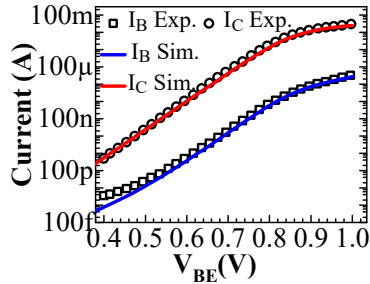


Fig. 2. Calibrated Gummel characteristics with experimental data at 300 K [8].

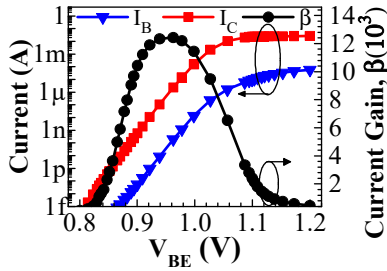


Fig. 3. Gummel characteristics with DC current gain (β) at temperature 77 K.

III. SIMULATION RESULTS AND DISCUSSION

We have investigated device characteristic from 300 K down to 41 K and investigated the performance with temperature variation. To validate our device design and further calculations, we calibrated SiGe HBT Gummel characteristics with experimental data with $V_{CE} = 0.85$ V at room temperature [8] as shown in Fig.2. Simulated data (line) has a good match with the experimental data (symbol) except in low base current regime in low V_{BE} .

At cryogenic temperatures under high electric field, energy exchange between the electron ensemble and the lattice temperature is reduced due to lower phonon population and this leads higher electron temperature [9]. We have achieved a record DC current gain (β) of 12,000 at $V_{BE} = 1.2$ V and $V_{CE} = 1.2$ V at 77 K. The advantage of bandgap engineering using graded Ge mole fraction in the SiGe base has also played a role in improving the performance of target HBT. This induces an intrinsic drift field in the base which improves the movement of the minority carriers (i.e. electron) transport toward collector side. Gummel characteristics for different cryogenic temperatures are shown in Fig. 4. It can be observed that the slope of collector current and base current strongly increases with decreasing temperature.

In order to capture the actual behaviour of collector current dependency on high frequency matrices cut-off frequency, output characteristics in saturation region and forward active region have been investigated. Fig. 5 shows the output characteristics ($I_C - V_{CE}$) at three different base current 2 μA , 4 μA and 6 μA for the temperatures 300 K, 77 K, 50 K and 41 K. In the forward active region, there is a slight increase in collector current with increasing V_{CE} . The slope of I_C in the

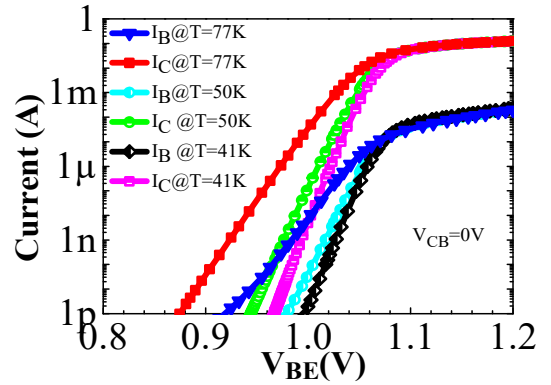


Fig. 4. Gummel characteristics at temperatures 41 K, 50 K and 77K.

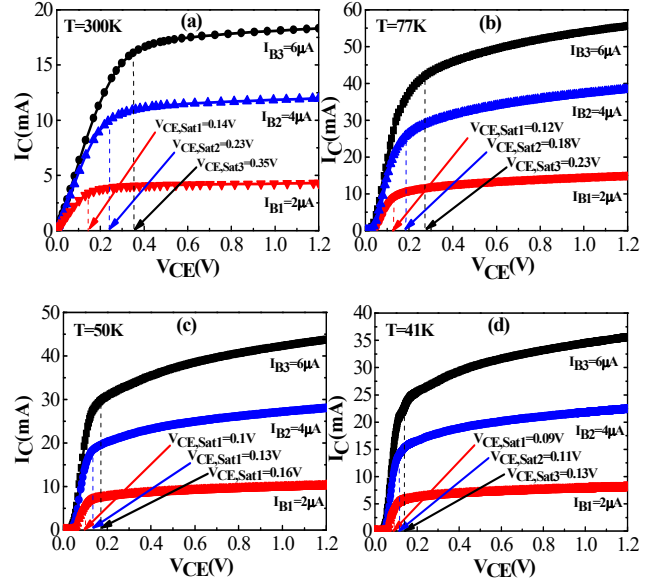


Fig. 5. Collector current (I_C (mA)) vs collector-emitter voltage (V_{CE} (V)) at three constant base current (I_{B1} , I_{B2} and I_{B3}) conditions for the temperatures (a) 300K, (b) 77 K, (c) 50 K and (d) 41 K.

forward active region increases, when the temperature goes down from 300 K to cryogenic temperature of 41 K, which indicates the non-zero finite output conductance with decreasing temperature. The output characteristics also indicates that the β of the transistor also increased at constant base current in forward active regime. In the saturation regime, collector current sharply increases with increasing V_{CE} from 0 to $V_{CE,Sat}$ with shifting V_{CE} window for saturation bias. In Fig. 5, for all the temperature conditions collector-emitter saturation voltage ($V_{CE,Sat}$) has been indicated with arrow.

The output characteristics simulation at cryogenic temperature (77 K, 50 K and 41 K) reveal that saturation bias regime shrinks with lowering of temperature. This saturation regime shrink has been gauged through $V_{CE,Sat}$ estimation, which lower with lowering of temperature for constant I_B . The $V_{CE,Sat}$ for different I_B should not vary much for a well-design bipolar junction transistor allowing lower V_{CE} window for forward active regime (FAR) accommodating large signal swing at output terminal. Hence, the SiGe HBT FAR performance enhancement is expected at cryogenic temperatures. The sharp drop in I_C in saturation regime with V_{CE} lowering at cryogenic temperature is attributed to less steeper net electron concentration gradient in quasi-neutral base. The extracted temperature coefficients of $V_{CE,Sat}$ from Fig. 6 are -0.16, -0.39, -0.75 mV/K for base currents 2, 4, 6 μA respectively.

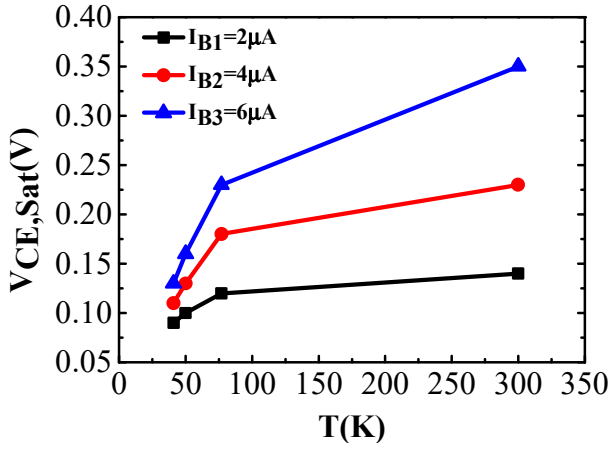


Fig. 6. $V_{CE,Sat}$ variation with temperature for three different base currents.

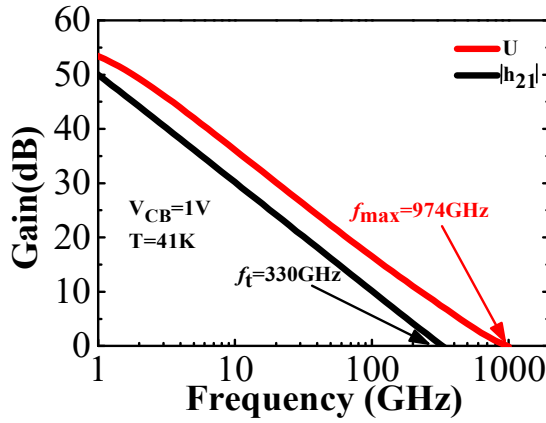


Fig. 7. Small-signal ac gain (dB) vs frequency (GHz) plot at temperature of 41 K : ac current gain (h_{21}) black line and ac power gain (U) red line.

Bode magnitude plots of small-signal current gain (h_{21}) and unilateral power gain (U) can be used to extract the cut-off frequency (f_t) defined in [11] at $|h_{21}|=1$ and maximum oscillation frequency (f_{max}) defined at $U=1$ with -20 dB per decade respectively.

$$f_t \equiv f(|h_{21}|=1=0[\text{dB}]) \quad (1)$$

$$f_{max} \equiv f(U=1=0[\text{dB}]) \quad (2)$$

At the temperature of 41 K, the obtained cut-off frequency (f_t) and maximum oscillation frequency (f_{max}) are 330 GHz and 974 GHz as obtained from (1) and (2) respectively as shown in Fig. 7. The ideal expression [12] of bipolar transistors for cut-off frequency (f_t) and maximum oscillation frequency (f_{max}) are,

$$f_t = \frac{1}{2\pi \left(\tau_f + \frac{kT}{qI_c} (C_{je} + C_{jc}) \right)} \quad (4)$$

$$f_{max} = \sqrt{\frac{f_t}{8\pi C_{jc} r_b}} \quad (3)$$

Where, forward transit time (τ_f), collector-base junction capacitance (C_{jc}), emitter-base capacitance (C_{je}), charge (q),

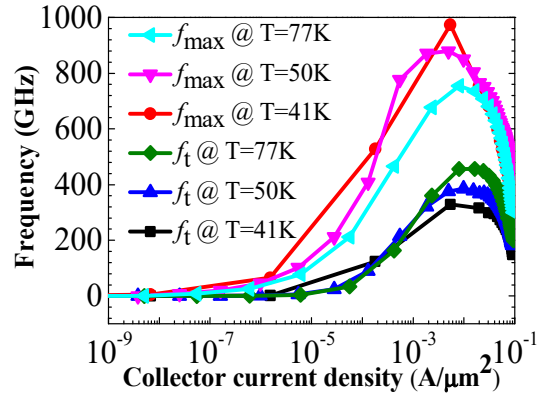


Fig. 8. Frequency (GHz) w.r.t. collector current density ($A/\mu m^2$) for cut-off frequency (f_t) and maximum oscillation frequency (f_{max}) at temperatures 41 K, 50 K and 77 K.

TABLE II. TCAD SIMULATION OF SIGE HBT PERFORMANCE MATRICES.

Temperature (K)	Peak f_t (GHz)	Peak f_{max} (GHz)
77	460	760
50	385	875
41	330	974

temperature (T) and Boltzmann-constant (k) are dependent parameters in determining cut-off frequency (f_t) in shown in (3). Maximum oscillation frequency (f_{max}) can be explain in terms of f_t , collector-base junction capacitance (C_{jc}) and the base resistance (r_b) in (4).

The effect of Ge incorporation in $Si_{1-x}Ge_x$ base leads lowering the conduction band edge, where as holes have larger barrier to surmount from the base side to the emitter side as compare to electron from emitter side to base side. It decides emitter injection efficiency of electron into the base. The combination of linearly graded Ge profile, which induces intrinsic drift field in the base (reduced base transit time (τ_{tb})) and cooling the HBT device result in enhancement of both f_t and f_{max} versus collector current density at temperatures 77 K, 50 K and 41 K and the results are shown in Fig. 8.

On the reduction in the lattice temperature, both the collector-base junction capacitance (C_{jc}) and the base resistance (r_b) significantly reduced which has improvement on peak f_{max} values. The f_t and f_{max} were evaluated at a constant collector drive current which required higher V_{BE} at lower temperatures. This is due to lower intrinsic carrier concentration at lower device temperature and requires a higher V_{BE} to maintain constant collector drive current. We have also performed simulation based study for f_t and f_{max} .

The observed peak of f_{max} increases with lattice cooling due to reduced device parasitic capacitances, where as the peak f_t is decreased below 100 K due to increase in emitter-base capacitance (C_{je}). This is due to reduction in emitter-base depletion width during the operation [4], which leads to increasing the junction capacitance. From (3), we observed that f_t has direct dependent on I_c , which shows continuous decrement in the collector current in low temperature analysis, which predicts that the f_t decreases for temperatures below 100K as shown in Fig. 9. The aggregate metric for peak value of $f_t + f_{max} > 1.2$ THz is achieved for the temperature values of 77 K, 50 K and 41 K under the cryogenic condition without scaling the device dimensions.

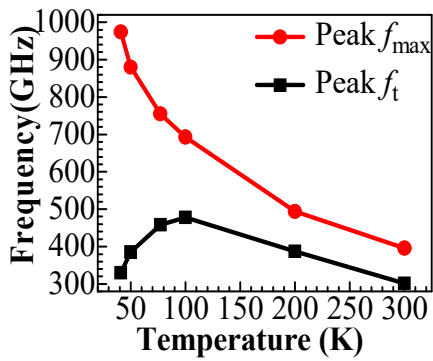


Fig. 9. Variation of peak value of cut-off frequency (Peak f_t) and maximum oscillation frequency (Peak f_{max}) in GHz w.r.t. temperature (K).

IV. CONCLUSION

In summary, device lattice cooling is an effective way for improving the performance of SiGe HBT without scaling device geometry. We have investigated the DC and small-signal performances of SiGe HBT device in cryogenic conditions. The performance of the SiGe based HBT is further improved by using bandgap engineering with linearly graded Ge molefraction in the base region. With these conditions, we have achieved a very high value of DC current gain (~ 12000) at 77 K. As we reduced the temperature, both collector junction capacitance and base resistance reduces, which has a significant impact on peak f_{max} values. Our simulations have also shown that peak f_{max} of about 974 GHz can be achieved at a temperature of 41 K. The peak f_t decreases for temperatures below 100 K due to increase in emitter junction capacitance. Finally, the aggregate performance metric $f_t + f_{max} > 1.2$ THz is achieved under cryogenic conditions.

ACKNOWLEDGMENT

The authors would like to thank the Electron Devices Research Laboratory (EDR Lab) members of the department of Electrical Engineering, Indian Institute of Technology Hyderabad for their valuable discussions and feedback. This work was supported by Council of Scientific & Industrial Research (CSIR), India.

REFERENCES

[1] P. S. Chakraborty, A. S. Cardoso, B. R. Wier, A. P. Omprakash, J. D. Cressler, M. Kaynak, and B. Tillack, "A 0.8 THz f_{MAX} SiGe HBT operating at 4.3 K," *IEEE Electron Device Lett.*, vol. 35, no. 2, pp. 151–153, 2014.

[2] J. C. Bardin, "Silicon-Germanium Heterojunction Bipolar Transistors For Extremely Low-Noise Applications," Ph.D. dissertation, California Inst. Technol., Pasadena, CA, USA, 2009.

[3] H. Ying, B. R. Wier, J. Dark, N. E. Lourenco, L. Ge, A. P. Omprakash, M. Mourigal, D. Davidovic, and J. D. Cressler, "Operation of SiGe HBTs Down to 70 mK," *IEEE Electron Device Lett.*, vol. 38, no. 1, pp. 12–15, jan 2017.

[4] Cressler, John D., and H. Alan Mantooth, eds. *Extreme environment electronics*. CRC Press, 2017.

[5] H. Rucker, B. Heinemann, and A. Fox, "Half-terahertz SiGe BICMOS technology," in *12th Topical Meeting on Silicon Monolithic Integrated Circuits in RF Systems (SiRF)*, 2012, pp. 133–136.

[6] B. Heinemann, H. Rucker, R. Barth, F. Bärwolf, J. Drews, G. G. Fischer, A. Fox et al. "SiGe HBT with f_x/f_{max} of 505 GHz/720 GHz." In *2016 IEEE International Electron Devices Meeting (IEDM)*, pp. 3-1. IEEE, 2016.

[6] S. Weinreb, J. Bardin, and H. Mani, "Design of Cryogenic SiGe LowNoise Amplifiers," *IEEE Trans. Microw. Theory Tech.*, vol. 55, no.11, pp. 2306–2312, nov 2007.

[7] *Sentaurus Device User Guide, Version P-2019.03*, Synopsys, Mountain View, CA, USA, 2017.

[8] F.M. Puglisi, Luca Larcher, and Paolo Pavan. "Mixed-mode stress in silicon-germanium heterostructure bipolar transistors: Insights from experiments and simulations." *IEEE Transactions on Device and Materials Reliability* 19, no. 2 (2019): 275-282.

[9] Hanbin Ying, Jason Dark, Anup P. Omprakash, Brian R. Wier, Luwei Ge, Uppili Raghunathan, Nelson E. Lourenco et al. "Collector transport in SiGe HBTs operating at cryogenic temperatures." *IEEE Transactions on Electron Devices* 65, no. 9 (2018): 3697-3703.

[10] P. S. Chakraborty, A. S. Cardoso, B. R. Wier, A. P. Omprakash, J. D. Cressler, M. Kaynak, and B. Tillack, "A 0.8 THz f_{MAX} SiGe HBT operating at 4.3 K," *IEEE Electron Device Lett.*, vol. 35, no. 2, pp. 151–153, 2014.

[11] "Sentaurus visual user guide, version P-2019.03," Synopsys, 2019.

[12] Peter Ashburn, *SiGe heterojunction bipolar transistors*. New York: John Wiley & Sons, 2003.

[13] Niccolò Rinaldi, and Michael Schröter, eds. *Silicon-Germanium heterojunction bipolar transistors for mm-wave systems: technology, modeling and circuit applications*. River Publishers, 2018.

[14] S. K. Mandal, G. K. Marskole, K. S. Chari, and C. K. Maiti. "Transit time components of a SiGe-HBT at low temperature." In *2004 24th International Conference on Microelectronics (IEEE Cat. No. 04TH8716)*, vol. 1, pp. 315-318. IEEE, 2004.

[15] Michael Schröter, Tommy Rosenbaum, Pascal Chevalier, Bernd Heinemann, Sorin P. Voinigescu, Ed Preisler, Josef Böck, and Anindya Mukherjee. "SiGe HBT technology: Future trends and TCAD-based roadmap." *Proceedings of the IEEE* 105, no. 6 (2016): 1068-1086.

[16] Nicolas Zerounian, Eloy Ramirez Garcia, Frédéric Aniel, Pascal Chevalier, Boris Geynet, and Alain Chantre. "SiGe HBT featuring $f_T > 600$ GHz at cryogenic temperature." *ECS Transactions* 16, no. 10 (2008): 1069.

[17] Mathieu Jaoul, David Ney, Didier Céli, Cristell Maneux, and Thomas Zimmer. "Analysis of a failure mechanism occurring in SiGe HBTs under mixed-mode stress conditions." In *2019 IEEE 32nd International Conference on Microelectronic Test Structures (ICMTS)*, pp. 33-37. IEEE, 2019.